Title

VISCOUS GLIDE, DISLOCATION CLIMB AND NEWTONIAN VISCOUS DEFORMATION MECHANISMS DURING HIGH TEMPERATURE CREEP IN Al-3 Mg

Author

Murty, K. Linga.

Publication Date

1971-12-01

Submitted to
Acta Metallurgica

LBL-442
Preprint

c.1

VISCOUS GLIDE, DISLOCATION CLIMB AND NEWTONIAN VISCOUS DEFORMATION MECHANISMS DURING HIGH TEMPERATURE CREEP IN Al-3 Mg

K. Linga Murty, F. A. Mohamed and J. E. Dorn

December 1971

AEC Contract No. W-7405-eng-48

LBL-442

DISCLAIMER

LBL-442

VISCOUS GLIDE, DISLOCATION CLIMB AND NEWTONIAN VISCOUS DEFORMATION MECHANISMS DURING HIGH TEMPERATURE CREEP IN Al-3 Mg

by

K. Linga Murty*, F. A. Mohamed** and J. E. Dorn†
Inorganic Materials Research Division
Lawrence Berkeley Laboratory
University of California, Berkeley, California

ABSTRACT

High-temperature creep has been studied in Al-3Mg solid solution alloy in the stress range of 10^{-6}G to 10^{-3}G using double-shear type specimens in a range of temperatures to near the melting point. A composite plot of dimensionless parameters $\dot{\gamma}$ kT/DGb versus τ/G indicated three distinct regions: region I extending from stresses of about 6 x 10^{-5} G and above, region II from 10^{-5}G to 6 x 10^{-5}G and region III below 10^{-5}G. Plots of logarithm of modulus-compensated strain-rate versus reciprocal of the absolute temperature in all the three regions yielded an average value of 33 k Cal/mole for the activation energy for creep. This value is in essential agreement with the activation energy for self-diffusion. Values for the stress exponents were found to be 3.2, 4.1 and 0.9 respectively in regions I, II and III. Viscous glide and dislocation climb mechanisms were found to be operative in regions I and II respectively. Present

*Research Associate

**Research Assistant

†Senior Scientist, and Professor of Materials Science of the College of Engineering, University of California, Berkeley, California; deceased September 1971.

experimental results in region III agreed very closely with the earlier data on pure Al in this normalized stress range. Modified versions of models based on jogged screw dislocation and/or climb of jogged edge dislocation were found to explain the present experimental results on Al-3Mg as well as the earlier data on Al. Experimental results were compared, in addition, with various theories of creep, and Nabarro, Coble, Nabarro-Herring in subgrains as well as Nabarro-Bardeen-Herring creep mechanisms were found to make at most a minute contribution to the overall creep-rate.

INTRODUCTION

A recent survey by Bird, Mukherjee and Dorn (hereafter referred to as BMD)[1] concluded that the steady-state rate of creep of a metal deforming at high temperature through any diffusion controlled mechanism is given by the dimensionless relation

$$\frac{\dot{\gamma} kT}{DGb} = A \left(\frac{\tau}{G}\right)^n \quad . \tag{1}$$

In this equation $\dot{\gamma}$ is the steady-state strain-rate, D the appropriate diffusivity, G the shear modulus, b the Burgers vector, τ the applied shear stress, A and n are constants depending upon the particular operating mechanism and kT has the usual meaning of Boltzmann's constant times the absolute temperature.

At high temperatures ($\gtrsim 0.5\ T_m$) creep in metals is controlled by dislocation climb. In such cases A has a mean value of 6×10^7 and the parameter n takes a range of values depending on the crystal structure. For fcc metals n lies in the range 4.2 to 5.5 and increases with Gb/Γ where Γ is the stacking fault energy. For bcc metals n lies in the range 4.0 to 5.5, and is near 4.5 in the majority of cases. For hcp metals, n is between 3.0 and 5.5. In solid solution alloys such as Al-Mg, creep is controlled by viscous glide motion of dislocations whenever dislocation climb is rapid, and these alloys display values of n from 3 to 3.6 in such cases.[2] Any interaction mechanism that can reduce the rate of gliding of dislocations to a value which is so low that glide becomes slower than dislocation-climb recovery, can produce such a creep behavior. For example, glide can proceed no faster than the rate of

solute-atom diffusion when these solute atoms are bound to dislocations through the Cottrell, Suzuki or analogous interaction mechanisms. Thus although climb always occurs in alloys, viscous glide mechanism controls the creep whenever the creep rate for glide is below that for the climb controlled mechanism. Such behavior has been observed in various solid solution alloys at stresses higher than about $10^{-5}G$.[3-6]

BMD suggested on theoretical grounds[1] that the dislocation-climb mechanism will prevail at lower stresses, though experimental verification of such a transition was then unavailable. The present research was undertaken to test this prediction. We studied the creep of Al-3Mg solid solution over a range of stresses to $10^{-6}G$ and a range of temperatures to near the melting point. The transition in creep mechanism predicted by BMD occurs in this alloy. In addition, a third creep mechanism was found to govern creep at low stresses. This mechanism is phenomenologically identical to that previously found by Harper and Dorn[7] in studies of creep in pure aluminum. The details of this mechanism are unknown.

EXPERIMENTAL PROCEDURE

Al-3Mg alloy was supplied by Kaiser Aluminum and Chemical Corporation. The final produce contained the following elements in atomic percent: Mg - 3.29, Si - 0.003, Fe - 0.003, Mn - 0.006, Cu - 0.005, Cr < 0.001, Zn - 0.003, Ti - <0.005. The remainder is Al. The cast ingots were soaked at 950°F for 48 hours and air cooled. After scalping ~0.2" per surface they were flash heated to 775°F and stablilized at that temperature for about an hour. The ingots initially measuring about 3 1/4"

thick were hot rolled to a final thickness of 0.875" in five passes. Double-shear specimens of the shape and dimensions shown in Fig. 1 (inset) were prepared from the rolled stock. Thus machined specimens were annealed in situ for a minimum of 2 hours at a temperature slightly above the planned test temperature prior to testing.

Tests were carried out either on an Instron testing machine or on a suitably designed creep machine at constant load; for this specimen configuration, constant load implies constant stress. The tests were conducted in air in an electric furnace. Temperatures were monitored with Chromel-Alumel thermocouples held in direct contact with the specimen (Fig. 1) and were held constant to better than $\pm$ 1° by a proportional controller. Length changes during the creep tests were measured by a Daytronic LVDT accurate to $\pm$ 5 x 10^{-5} in. Tension tests were performed on an Instron machine using selected strain-rates at fixed temperature (Fig. 1). By using double-shear type test specimens, uniform elongations and constant steady-state strain-rates were observed to shear strains beyond 0.80.[8] Whenever required, grain size measurements were carried out by chemical polishing and etching, and revealed that grain size is 3 $\pm$ 1 mm for 24 hours anneal at 863°K.

EXPERIMENTAL RESULTS

As noted in the earlier section, data were obtained through both creep and Instron tests. Differential stress and strain-rate tests were employed on the creep and Instron machines respectively. In both these cases the specimens were left to achieve the steady state before changing the stress or the strain-rate. The data obtained are plotted in Fig. 2

as $\ln \frac{\dot{\gamma}kT}{DGb}$ versus $\ln \frac{\tau}{G}$ with $D = 0.45 \exp\left(-\frac{33000}{RT}\right)$. The choice of the value of 33 k Cal/mole for the activation energy for self-diffusion was based on the creep activation energy obtained in the present study, as will be seen later. This value, nevertheless, is nearly equal to the self-diffusion value obtained by NMR[9] and tracer[10] techniques in pure Al. The unavailability of inter-diffusivity data on Al-Mg solid solutions forced the choice of the value of 0.45 for D_o corresponding to that for self-diffusion in pure Al. The effect of these choices will be discussed later. The shear stresses employed range from about $2 \times 10^{-6}G$ to $10^{-3}G$. The equivalence of the creep and tension testing is apparent from the overlap of the datum points obtained from these tests (Fig. 2). The lowest available cross head speed of the machine restricted the data to stresses greater than or equal to about $4 \times 10^{-5}G$. Three distinct regions appear in Figure 2: region I extending from stresses of about $6 \times 10^{-5}G$ and beyond, region II from $10^{-5}G$ to $6 \times 10^{-5}G$ and region III below $10^{-5}G$. The values of n and A obtained in these 3 regions are tabulated in Table I.

The temperature dependence of the steady-state creep rate was studied in each of the three regions. Effective activation energies were obtained from the slopes of the Arrhenius plots shown in figures 3a, 3b and 3c. Fig. 3a shows plots of '$\ln \dot{\gamma} G^2 T$ vs $1/T$' at constant stresses of 300 and 600 psi. These data fall in region I and give a value of 33.10 ± 2.16 k Cal/mole for the activation energy. '$\ln \dot{\gamma} G^3 T$ vs $1/T$' is plotted for region II in Fig. 3b. These data yield a value of 31.08 ± 0.52 k Cal/mole for the activation energy for creep. A similar plot for the region III is presented in Fig. 3c where $\ln \frac{\dot{\gamma}T}{\tau}$ is plotted against $1/T$ since temperature variation in this region covers only a small range.

The line drawn through the datum points yields a value of 35.70 ± 5.78 k Cal/mole. These three values for the effective activation energies for creep are also included in Table 1. An average value of 33 k Cal/mole was obtained for the activation energy and this was used in plotting Fig. 2.

Important differences were noted in the creep curves corresponding to various regions. Fig. 4 is a schematic representation of the important features of the curves observed in the three regions.

Creep curves in region I are typical of solid solution alloys with no extensive initial strain upon loading. They are characterized by brief transient creep, indicating that the substructure pertinent to creep remains substantially constant. Additional support of these findings is obtained through intermittant loading experiments. In one of the tests the specimen was unloaded after it crept to a certain strain in the steady state and left for about 3 hours at the test temperature. Upon reloading to the original stress the steady state was achieved immediately and no transient was observed (Fig. 5a). It may be noted that sometimes inverted creep curves may be observed in the viscous glide region.[1] An example is shown in Fig. 5b for Al-5 Mg where normal primary creep was observed before deformation while inverted curves were observed after deformation[11]. In no case were such inverted transients found in the present study of Al-3 Mg.

In contrast to these observations extensive normal primary creep regions were noted for specimens crept in region II. The decelerating primary creep rate illustrates the continued formation of a more creep

resistant substructure during the transient stage. When the stress was removed and reapplied after an hour, a region of primary creep was again observed following a small instantaneous strain (Fig. 6). However the final steady-state creep rate was exactly the same as the original value. These results resemble the observations made by Raymond et al[12] on creep of pure Al.

Creep curves obtained in the viscous creep region (region III here) are similar to curves obtained previously from tests of pure Al in the same stress range.[7] The transients observed in the annealed samples were present even after prior deformation.

It is to be noted that in all the intermittant-stress tests, immediate transients accompanying changes in stress[13] are not depicted. The details of these transients form an entirely different study and will be the subject of a future publication.

DISCUSSION

The transition from region I ($n \sim 3$) to region II ($n \sim 4$) at a stress of about $6 \times 10^{-5} G$ (depicted in Fig. 2) apparently confirms the theoretical prediction by BMD[1] of a transition from viscous glide to climb regions. In order to provide background for the discussion on the theoretical implications of the presently documented high-temperature creep data on Al-3 Mg alloy, a brief outline will be presented on the various creep theories that have been proposed.

Excluding a few rare exceptions metals and alloys deform by diffusion-controlled creep at low stresses and high temperatures (above about one-half of the melting point). The various diffusion controlled creep

mechanisms documented in Table II have been suggested[1,14].

Among the listed mechanisms, Nabarro,[16] Coble,[17] and perhaps Superplastic[1] creep as well, are due to changes in grain shape arising directly from vacancy fluxes under chemical-potential gradients. In contrast creep by the climb[18] and viscous glide[2] mechanisms are due to average rates of slip displacements of dislocations released by climb. At the steady state a balance must necessarily be obtained between the rate of accumulation of dislocations and their rate of removal by climb-recovery. To account for continuing steady-state creep, recovery by dislocation climb must always be operative at high temperatures.[14] In solid solution alloys however, as noted earlier, although climb always occurs the creep rate is controlled by viscous glide motion of dislocations when it gives the slower rate. Jogs on screw dislocations may impede the conservative motion of the dislocations and further slip is possible only by the nonconservative motion of these jogs in the direction of the advance of screw dislocations.[19-22] As noted by Dorn et al[15] this mechanism needs extensive improvements and the problem becomes extremely difficult because of moving sources, ill-defined boundary conditions and competition between pipe and volume diffusion, types of jogs, jog-jog interactions, effects of dissociation etc. Thus a mechanism based on some kind of edge dislocation climb is preferred over the jogged screw dislocation mechanism. Since dislocation glide and climb are mutually exclusive the total creep rate in solid solutions is due to the rates ascribable to either climb or viscous glide, dependent on which is controlling, plus the sum of rates from all remaining mechanisms. As will be clear, although many mechanisms can be operable at one time,

usually one exhibits the highest creep rate and therefore becomes dominant over special ranges of τ/G and T. Transient creep seems to occur only when dislocation cells and entanglements are produced as a result of the initial plastic straining that takes place upon the application of stress.[23] In the absence of initial plastic straining, however, the steady-state creep rate is achieved almost immediately following stressing. Obviously Nabarro, Coble and Superplastic creep mechanisms do not exhibit transient stages. This is also true for the recently proposed Nabarro-Bardeen-Herring[24] mechanism based on climb of dislocations from Bardeen-Herring sources.

With this introduction on the various creep mechanisms we proceed to correlate the present experimental results with the thus far documented theories. Since the activation energy for creep in the 3 regions is 33 k Cal/mole and is about the same as that for self-diffusion in aluminum, the mechanisms B(b), E and F (Table II) can be immediately omitted from further discussion. The very fact that at higher stresses (Region I) a smaller n value ($\sim$ 3 compared to $\sim$ 4 of region II) was observed indicates that the mechanisms responsible for the regions I and II act in series and are exclusive. The added observation of the equality of the activation energies for creep in both regions with that for self-diffusion leaves no doubt that viscous glide motion of dislocations and dislocation-climb control creep in I and II respectively. To correlate the present experimental results on Al-3Mg with various theoretical predictions, the experimental data are plotted in Fig. 7 along with the theoretical lines.

Region I: A value of 3.2 for n in this stress-range discounts the possibility of climb (A) and Nabarro (D) creep mechanisms. Further

elimination is achieved through the pre-exponential factor 'A'. The experimental value of A (Table I) refutes B (a) as the controlling mechanism since even if l_j is taken conservatively as '10b', this factor is too large compared to 47 while the Nabarro-Subgrain and N-B-H mechanisms can be ruled out since they predict too small a value for A. In addition it is questionable on theoretical grounds whether the Nabarro creep in subgrains and N-B-H creep can ever take precedence over viscous glide and/or climb mechanisms.[1] This isolates the Viscous Glide mechanism and the experimental results are in line with the predictions based on this model. As to be noted, the expression for the creep-rate presented here for glide was taken from BMD and this differs slightly from Weertman's,[6] in that the latter theory predicts solute-concentration-dependence of the pre-exponential factor.* Moreover such an expression can be derived in a more straightward and elegant way as given below.[1] For the case where all dislocations within a crystal drag Cottrell atmosphere, the shear strain-rate is given by [25]

$$\dot{\gamma} = \rho b v = \rho b \left(\frac{\nu b}{\lambda}\right) b \exp\left(-\frac{g_d}{kT}\right) \left\{\exp\left(\frac{\tau \lambda b^2}{kT}\right) - \exp\left(\frac{-\tau \lambda b^2}{kT}\right)\right\} \quad (2)$$

where v is the dislocation velocity, ν the Debye frequency and g_d the free energy of activation for solute atom diffusion. Since $\tau \lambda b^2 << kT$ and $D = \nu b^2 \exp(-g_d/kT)$,

$$\dot{\gamma} = 2 \rho D \frac{\tau b^3}{kT} \quad (3)$$

*Whereas the experimental results on Al-5 Mg also yielded identical values for A and n as on Al-3 Mg.[11]

It is important to note that the proper diffusivity applicable here is the chemical interdiffusivity of the alloy as given by the Darken expression for binary solutions,

$$\tilde{D} = (N_A D_B^* + N_B D_A^*)\left(1 + \frac{\partial \ln \gamma_A}{\partial \ln N_A}\right) \quad , \qquad (5)$$

where N_A and N_B are the atomic fractions of A and B atoms, D_A^* and D_B^* are the tracer diffusivities of the A and B atoms in the AB alloy and γ_A is the activity coefficient of the A species. The paucity of data on the chemical interdiffusivity and the activity coefficient makes accurate correlation of the expression with the present experimental findings difficult. However as noted by BMD this should not make too much difference in the present case of Al-Mg solid solution alloy. As is clear from Table I and Fig. 7, experimental results in region I correlate well with Eq. 4.

Region II: Experimental values for the pre-exponential factor and the stress exponent point to the climb mechanism. The expression given in Table II for the climb-creep was taken from BMD obtained from a correlation of available experimental data on various metals and alloys and neither the existing theories based on the pile up models,[18] dipole annihilation,[26] and modifications thereof[27,28] nor the relatively recent N-B-H creep[24] predict the correct exponent as well as the pre-exponential factor. Dorn et al[15] observed that although Chang's theory[26] based on dipole annihilation does not predict the correct values for n and A, it nevertheless has very attractive features and further modifications on these lines may prove invaluable. In lieu of correct theory we would

like to compare the present experimental results with the climb equation applicable to pure Al. Such a comparison is shown in Fig. 2 where it is clear that Al-Mg data fall below the Al curve and part of this discrepancy might have arisen from the diffusion frequency factor (D_o) since the appropriate diffusivity here is

$$D = \frac{D_A^* D_B^*}{(N_B D_A^* + N_A D_B^*)f} \quad , \tag{6}$$

in lieu of the simpler D^*/f for pure Al; here f is the correlation factor. Region III: In this stress range ($\frac{\tau}{G} \lesssim 10^{-5}$) $n = 0.91 \pm 0.03$ and $A = 2.88 \times 10^{-11}$. For the grain size of the Al-Mg samples of the present study, predictions based on Nabarro creep yield strain-rates smaller by 3 orders of magnitude than the experimental values. However present results fall very close to the aluminum data of Harper and Dorn[7] in this normalized stress range. These observations cannot be explained by any of the mechanisms tabulated in Table II. Mechanisms which predict viscous deformation such as Nabarro, Coble etc., fall orders of magnitude lower than the experimental results and, in addition they predict grain size dependence of the creep rate while Harper and Dorn[7] observed that single crystal data agree with those of polycrystalline. Moreover recent study by Muehleisen[29] on Al in this stress range clearly revealed subgrain formation indicating thereby slip due to dislocation motion. Appearance of large transient creep regions add to the above to refute the diffusional creep due to vacancy exchange as the controlling mechanism.

The high-temperature creep model based on Nabarro-Herring mechanism in subgrains[25] also fails to explain the present experimental results. Muehleisen[29] observed that, in this stress range, subgrain size tends

to be independent of the applied stress and reaches a constant value of about 1mm. Thus[1]

$$\left(\frac{\dot{\gamma}kT}{DGb}\right)_{\text{Nabarro-Subgrain}} = 12\left(\frac{b}{\delta}\right)^2\left(\frac{\tau}{G}\right) = 9.8 \times 10^{-13}\left(\frac{\tau}{G}\right) .$$

This model predicts strain rates which are two orders of magnitude lower than the experimental values.

Slight modifications of some of the creep theories seem to explain the observed n = 1 dependence, grain size insensitivity as well as the magnitude of A[29,30]. Consider for example the jogged screw mechanism, B(a) in Table II, according to which[19]

$$\frac{\dot{\gamma}kT}{DGb} = 6\,\rho_s l_j\, b\left(\frac{\tau}{G}\right) \quad . \tag{7}$$

Here, only vacancy absorbing jogs are considered since most of the jogs produced by athermal processes are of this type.[31] If the mobile screw dislocation density (ρ_s) is independent of the applied stress, the above equation predicts a linear stress-dependence of the creep rate. Recent x-ray topographic studies by Nost and Nes[32] reveal that at stresses of the order of 10^{-6}G, the dislocation density tends to remain independent of the stress and to acquire a constant value of the order of $10^3 - 10^4$ cm^{-2}. At higher stresses the density was proportional to the square of the applied stress as expected.[1] Muehleisen[29] attempted to show the same through etch pit and electron transmission microscopy techniques in crept Al at these small values of stress. Scatter in the data is too enormous to draw any quantitative conclusions although his data do seem to point to the constancy of ρ at these extreme stress values. Thus if ρ_s is assumed to be a constant, in the region III, equal to 10^4

cm^{-2} and if l_j is taken as equal to b[33] then the predicted value for A through Eq. 7 above comes out to be

$$A = 6 \rho_s l_j b = 4.7 \times 10^{-11}$$

while the experimental values are

$$A^{Al}_{Harper\text{--}Dorn} = 4.05 \times 10^{-11}$$

and

$$A^{Al\text{-}3Mg}_{Present} = 2.88 \times 10^{-11}$$

Such an excellent agreement is very encouraging and perhaps this modified jogged screw dislocation mechanism controls creep at these low stresses. If the present allegations are correct, such type of creep; referred to as Harper-Dorn creep; should be observable in all metals and should be a universal type such as climb at high stresses. Very recent experimental results in pure lead indicate such trends,[34] and experiments are in progress to observe such a creep mechanism in pure tin as well as copper also.[35] Muehleisen[29] failed to observe n=1 dependence in copper and copper-silicon alloys, and a re-evaluation of his data in terms of Eq. 1 indicates that his results extend to stress values equal to or higher than $5 \times 10^{-6} G$. As is obvious from the present work region III starts from about $10^{-5} G$ - $5 \times 10^{-6} G$ towards lower stresses and thus Muehleisen's results are inconclusive. This is one of the reasons to choose Cu for further study, in addition to finding the possible effect of stacking fault energy on the Newtonian viscous flow in metals.

As shown by Muehleisen,[29] this n=1 stress dependence may also be derived from climb models if ρ is assumed constant. Calculations by

Hirth and Lothe[36] yield the following expressions for models based on the climb motion of jogged edge dislocations

$$\left(\frac{\dot{\gamma} kT}{DGb}\right)_{\text{point}} = 12\,\pi\,\rho\,\frac{b^3}{\lambda}\left(\frac{\tau}{G}\right) \quad , \lambda >> b \tag{8a}$$

and

$$\left(\frac{\dot{\gamma} kT}{DGb}\right)_{\text{line/skew}} = 6\,\pi\,\rho\,\frac{b^2}{\ln\,(1/\sqrt{\rho}\lambda)}\left(\frac{\tau}{G}\right) \quad , \tag{8b}$$

where λ is the spacing of jogs. In Eq. 8b above, the subscript 'skew' corresponds to the case where the jogs appear as groups of segmented line sources on the dislocation with spacing λ, and if $\lambda \approx b$ the dislocation is regarded as a 'line' source. Thus if λ is taken as 50b in the 'point' and 'skew' cases,[36] following values are obtained for A in Eq. 1

$$A_{\text{point}} = \frac{6}{25}\,\pi\,\rho\,b^2 = 6.17 \times 10^{-12}$$

$$A_{\text{line}} = 6\,\pi\,\rho\,b^2/\ln\,(1/\sqrt{\rho}\,b) = 1.21 \times 10^{-11}$$

$$A_{\text{skew}} = 6\,\pi\,\rho\,b^2/\ln\,(1/\sqrt{\rho}\,50b) = 1.74 \times 10^{-11}$$

for $\rho = 10^4$ cm^{-2}. These values for A are of the same order as that obtained in the present experiments on Al-3Mg as well as that predicted by the modified model based on the motion of jogs on screw dislocations as seen earlier. Thus from the mechanical data alone, it is not possible to identify the controlling mechanism uniquely. Microstructural studies by transmission electron microscopy are needed to unravel this problem and such studies are presently underway[35].

Thus various features of the three regions depicted in Fig. 2 bring out the need for further experimental work, especially on substructures

developed in the deformed metals. Creep data presented here, however, predict important and significant differences in the dislocation structures developed in the viscous glide, dislocation climb and Newtonian viscous regions; for example, well defined subboundaries are expected to be found in the metals deformed in the climb region.

Fig. 7 summarizes the present experimental results and various theoretical predictions. As is clear from this plot, Nabarro-Herring, Coble, Superplastic, Nabarro-Herring in subgrains (both with $\delta = 10b\ (\tau/G)^{-1}$ and a constant value of 1mm)[1,29] and Nabarro-Bardeen-Herring mechanisms do not contribute significantly to the overall creep-rates in Al-3Mg in the stress range $\sim 10^{-6}$ to $\sim 10^{-3}$ G.

CONCLUSIONS

1. High-temperature creep data on Al-3Mg analyzed in terms of the dimensionless parameters $\frac{\dot{\gamma}kT}{DGb}$ and τ/G revealed three distinct regions when plotted as logarithm of compensated strain-rate versus logarithm of normalized stress. Values for the stress exponents in the three regions were found to be 3.2, 4.1 and 0.9 respectively in the high (I), intermediate (II) and low (III) stress regions.
2. A value of 33 k Cal/mole was obtained for the activation energy for creep in the three regions and this value is in good agreement with that for self-diffusion in pure aluminum.
3. Viscous glide and dislocation climb mechanisms were found to be operative in regions I and II respectively.
4. Present experimental results in region III agreed closely with the earlier data on pure aluminum. Although the τ^1 dependence of the

strain-rate points to diffusional creep mechanism by vacancy exchange such as Nabarro-Herring model, the experimental values are three orders of magnitude higher than the predictions based on these models.

5. The evidence suggests that at low stresses (region III) the dislocation density as well as the subgrain diameter are independent of the applied stress. Modified versions of the models based on jogged screw dislocation were found to explain the present experimental results as well as the earlier data on aluminum.

ACKNOWLEDGMENTS

This work was supported by the United States Atomic Energy Commission through the Inorganic Materials Research Division of the Lawrence Berkeley Laboratory of the University of California, Berkeley. The authors are thankful to Professor J. W. Morris, Jr., for his critical reading of the manuscript, valuable discussions and interest in the present research.

REFERENCES

1. J. E. Bird, A. K. Mukherjee and J. E. Dorn, "Correlations Between High-Temperature Creep Behavior and Structure," in Quantitative Relation Between Properties and Microstructure, Israel University Press, Jerusalem, p. 255-342 (1969).

2. J. Weertman, J. Appl. Phys., 28, 1185 (1957).

3. C. M. Sellars and A. G. Quarrell, J. Inst. Met., 90, 329 (1961-62).

4. H. Laks, C. D. Wiseman, O. D. Sherby and J. E. Dorn, J. Appl. Mech., 24, 207 (1957).

5. R. Horiuchi, H. Yoshinaga and S. Hama, Trans. Japan Inst. Met. 6, 123 (1965).

6. J. Weertman, Trans. AIME, 218, 207 (1960).

7. J. G. Harper and J. E. Dorn, Acta. Met. 5, 654 (1957).

8. D. M. Schwartz, J. B. Mitchell and J. E. Dorn, Acta. Met. 15, 485 (1967).

9. J. J. Spokas and C. P. Slichter, Phys. Rev. 113, 1462 (1962).

10. T. S. Lundy and J. F. Murdock, J. Appl. Phys. 33, 1671 (1962).

11. K. Linga Murty, F. A. Mohamed, and J. E. Dorn, unpublished work.

12. L. Raymond and J. E. Dorn, Trans. AIME, 230, 560 (1964).

13. C. N. Ahlquist and W. D. Nix, Scripta Met., 3, 679 (1969).

14. D. Klahn, A. K. Mukherjee and J. E. Dorn, "Strain-Rate Effects," in the 'Strength of Metals and Alloys,' 2nd International Conference, Asilomar, California (1970).

15. A. K. Mukherjee, J. E. Bird and J. E. Dorn, Trans. ASM, 62, 155 (1969).

16. F. R. N. Nabarro, Report of a Conference on the Strength of Solids, p. 75, The Physical Society, London (1948).

17. R. L. Coble, J. Appl. Phys. 34, 1679 (1963).

18. J. Weertman, J. Appl. Phys. 28, 362 (1957); also see Trans. ASM, 61, 681 (1968).

19. P. B. Hirsh and D. H. Warrington, Phil. Mag. 6, 735 (1961).

20. G. B. Gibbs, "Equilibrium Velocities of Defect-Emitting Jogs," RD/B N884, Berkeley Nuclear Laboratory, England (1967).

21. C. R. Barrett and W. D. Nix, Acta Met., 13, 1247 (1965).

22. K. Linga Murty, M. Gold and A. L. Ruoff, J. Appl. Phys. 41, 4917 (1970).

23. K. E. Amin, A. K. Mukherjee and J. E. Dorn, J. Mech. Phys. Solids, 18, 413 (1970).

24. F. R. N. Nabarro, Phil. Mag. 16, 231 (1967).

25. J. Friedel, "Dislocations," Pergamon Press, London (1964).

26. R. Chang, in "The Physics and Chemistry of Ceramics," Gordon and Breach, New York (1963).

27. R. W. Christy, J. Appl. Phys. 30, 760 (1959).

28. J. E. Bird, Ph.D Thesis, University of California, Berkeley, in progress.

29. E. C. Muehleisen, Ph.D. Thesis, Stanford University (1969).

30. J. E. Dorn and J. D. Mote, "Physical Aspects of Creep," in 'High Temperature Structures and Materials,' Pergamon Press, London (1963) p. 95.

31. J. Weertman, Trans. AIME, 233, 2069 (1965).

32. B. Nost and E. Nes , Acta Met. 17, 13 (1969).

33. John E. Dorn, private communication.

34. F. A. Mohamed, K. Linga Murty and J. E. Dorn, "High-Temperature - Low-Stress Viscous Deformation in pure Lead," to be published.

35. F. A. Mohamed and K. Linga Murty, research in progress.

36. J. P. Hirth and J. Lothe, "Theory of Dislocations," Mc Graw-Hill, New York (1968).

TABLE I

Experimental Values for Various Parameters in the three Regions

Region	ΔH k Cal/mole	n	A
I	33.10 ± 2.16	3.19 ± 0.03	46.77 ± 10.86
II	31.08 ± 0.52	4.05 ± 0.07	$(1.74 \pm 1.50) \times 10^{5}$
III	35.70 ± 5.78	0.91 ± 0.03	$(2.88 \pm 1.39) \times 10^{-11}$

TABLE II

Diffusion Controlled Creep Mechanisms

#	Mechanism	Relationship
A	Dislocation Climb	$\frac{\dot{\gamma}kT}{DGB} = 6 \times 10^{7} (\tau/G)^{4 \text{ to } 7}$
B	Jogged Screw Dislocation	$\frac{\dot{\gamma}kT}{DGB} = \frac{2\pi l_j}{b} (\tau/G)^3$ (a)
		$\frac{\dot{\gamma}kT}{D_c Gb} = \pi(\tau/G)^3$ (b)
C	Viscous Glide	$\frac{\dot{\gamma}kT}{DGb} = 6 (\tau/G)^3$
D	Nabarro-Herring	$\frac{\dot{\gamma}kT}{DGb} = 12 (b/d)^2 (\tau/G)$
E	Coble	$\frac{\dot{\gamma}kT}{D_b Gb} = 100 (b/d)^3 (\tau/G)$
F	Superplastic	$\frac{\dot{\gamma}kT}{D_b Gb} = \sim 200 (b/d)^2 (\tau/G)^2$
G	Nabarro-Subgrain	$\frac{\dot{\gamma}kT}{DGb} = 12 (b/\delta)^2 (\tau/G)$
		$(\delta/b) = 10 (\tau/G)^{-1}$
H	Nabarro-Bardeen-Herring	$\frac{\dot{\gamma}kT}{DGb} = \frac{1}{\pi \ln (4G/\pi\tau)} (\tau/G)^3$

(a) if jogs on the screw dislocation are all either vacancy emitting or absorbing type

(b) for the case when equal numbers of both types of jogs are present

D_c = Core Diffusivity

D_b = Grain Boundary Diffusivity

l_j = mean distance between jogs

d = mean grain diameter

δ = subgrain diameter

FIGURE CAPTIONS

1. A typical stress-strain curve during differential strain-rate tests in Al-3Mg. Inset shows the drawing of the double-shear type specimens.

2. Plot of $\ln \frac{\dot{\gamma}kT}{DGb}$ vs $\ln \frac{\tau}{G}$ depicting the three regions with slopes 3.2, 4.1 and 0.9 indicating the transitions from glide to climb and climb to Newtonian viscous creep mechanisms. Data of Harper and Dorn[7] on pure Al are included for comparison.

3a. Arrhenius plot of $\ln \dot{\gamma} G^2 T$ versus $1/T$ in region I. Slope of the line gives a value of 33.1 $\pm$ 2.2 k Cal/mole for the activation energy for creep.

3b. Plot of $\ln \dot{\gamma} G^3 T$ vs $1/T$ in region II at a constant stress. The value for the activation energy for creep was found to be 31.1 $\pm$ 0.5 k Cal/mole.

3c. Plot of $\ln \frac{\dot{\gamma} T}{\tau}$ versus $\frac{1}{T}$ in region III. The slope of the line yields a value of 35.7 k Cal/mole for the activation energy for creep.

4. Schematic representation of the creep curves observed in the three regions.

5a. Typical intermittant-stress test in region I showing no or brief transients after reloading.

5b. Same as Fig. 5a except in Al-5Mg depicting the observation of inverted primary creep after reloading.[11]

6. Intermittant-stress test in region II showing the existence of normal primary creep even after prior deformation.

7. Plot of $\ln \frac{\dot{\gamma}kT}{DGb}$ vs $\ln \frac{\tau}{G}$. Various theoretical lines are plotted for comparison with the experimental results on Al-3Mg.

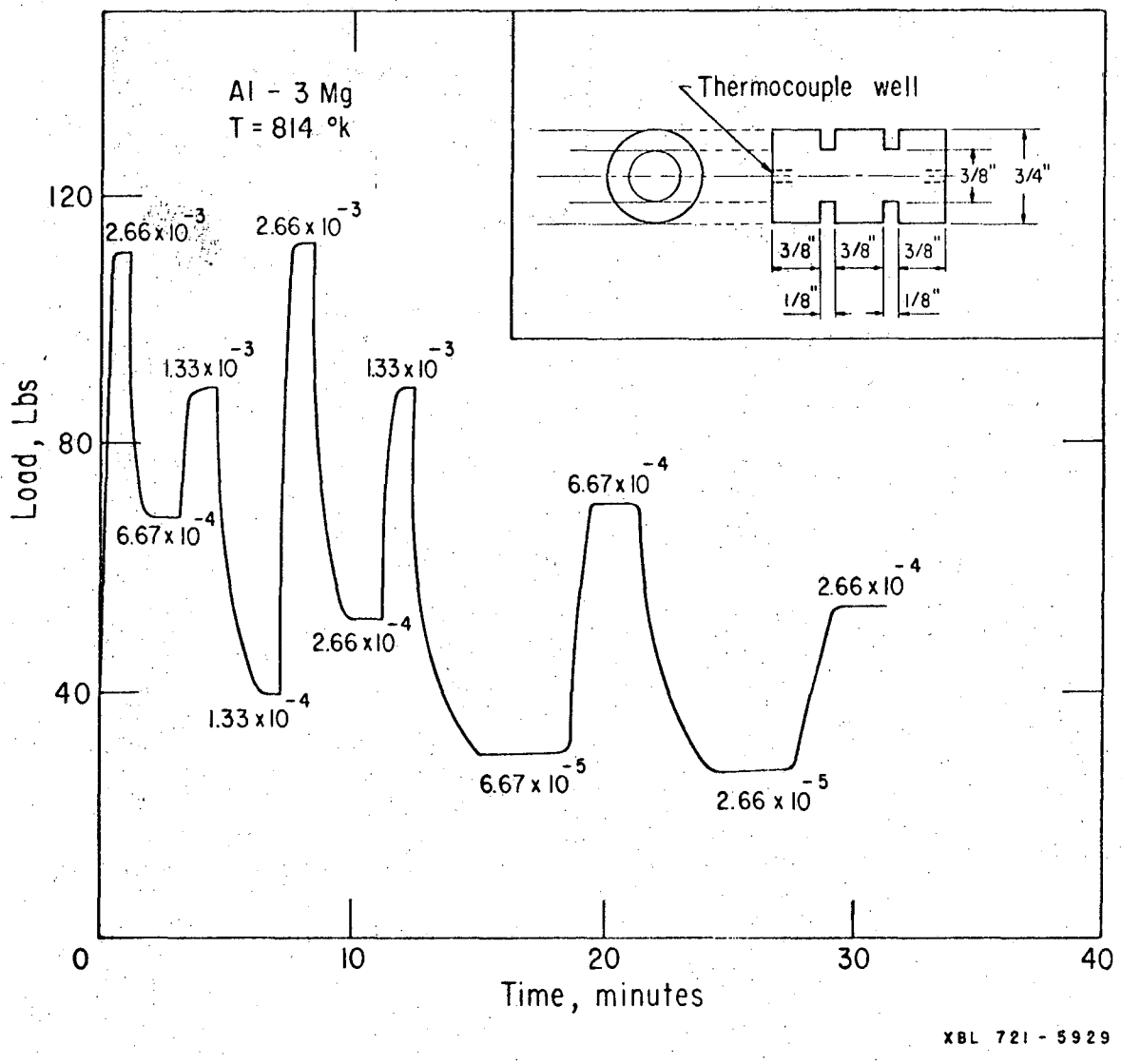
Al - 3 Mg
T = 814 °k
Thermocouple well
3/8"
3/4"
3/8"
3/8"
3/8"
1/8"
1/8"
120
80
40
0
10
20
30
40
Load, Lbs
Time, minutes
2.66 x 10^-3
2.66 x 10^-3
1.33 x 10^-3
1.33 x 10^-3
6.67 x 10^-4
1.33 x 10^-4
2.66 x 10^-4
6.67 x 10^-4
2.66 x 10^-4
6.67 x 10^-5
2.66 x 10^-5
XBL 721 - 5929

Fig. 1

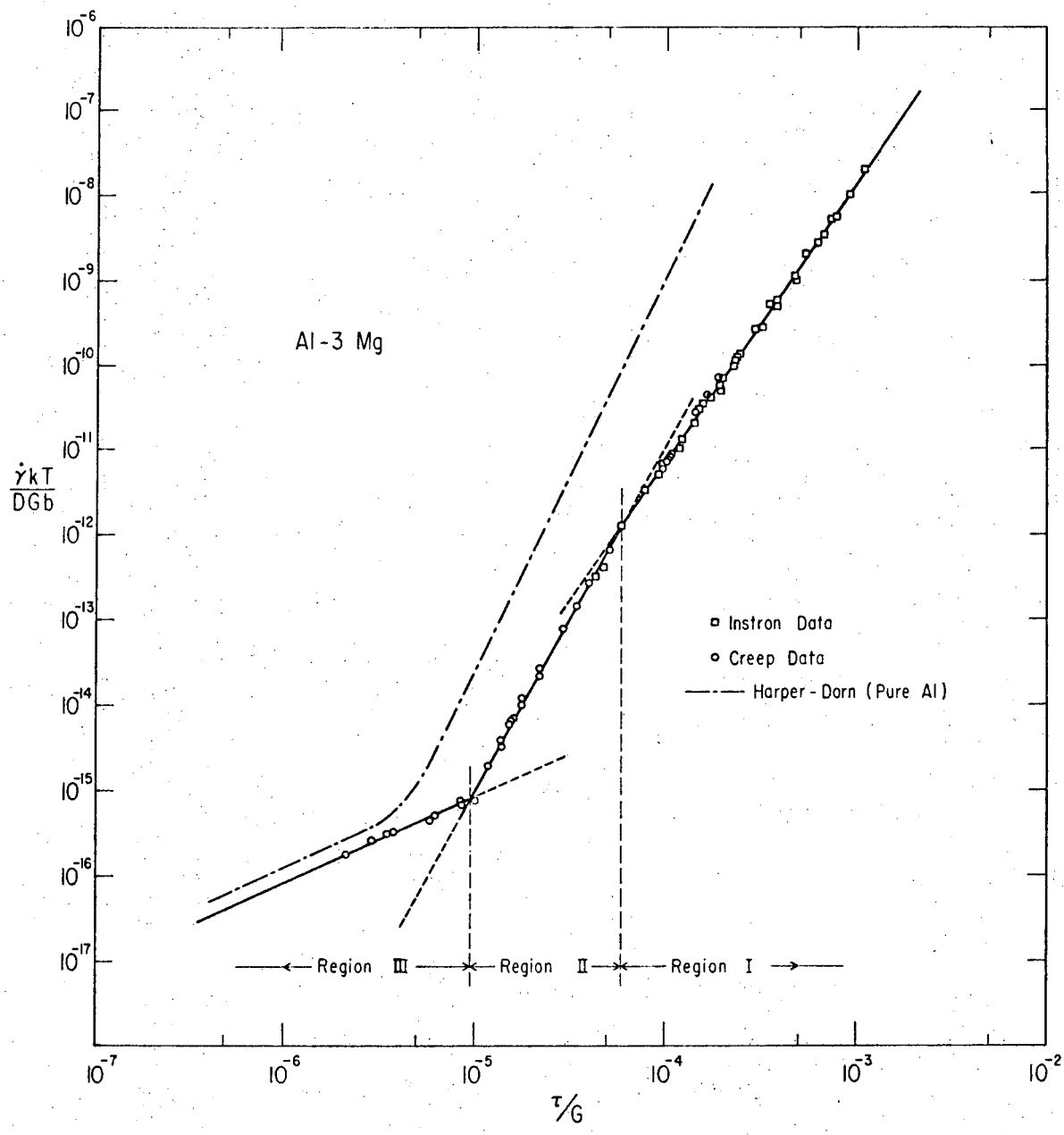
Al-3 Mg
Instron Data
Creep Data
Harper-Dorn (Pure Al)
Region III
Region II
Region I
$\frac{\dot{\gamma}kT}{DGb}$
τ/G
XBL 7112-2304

Fig. 2

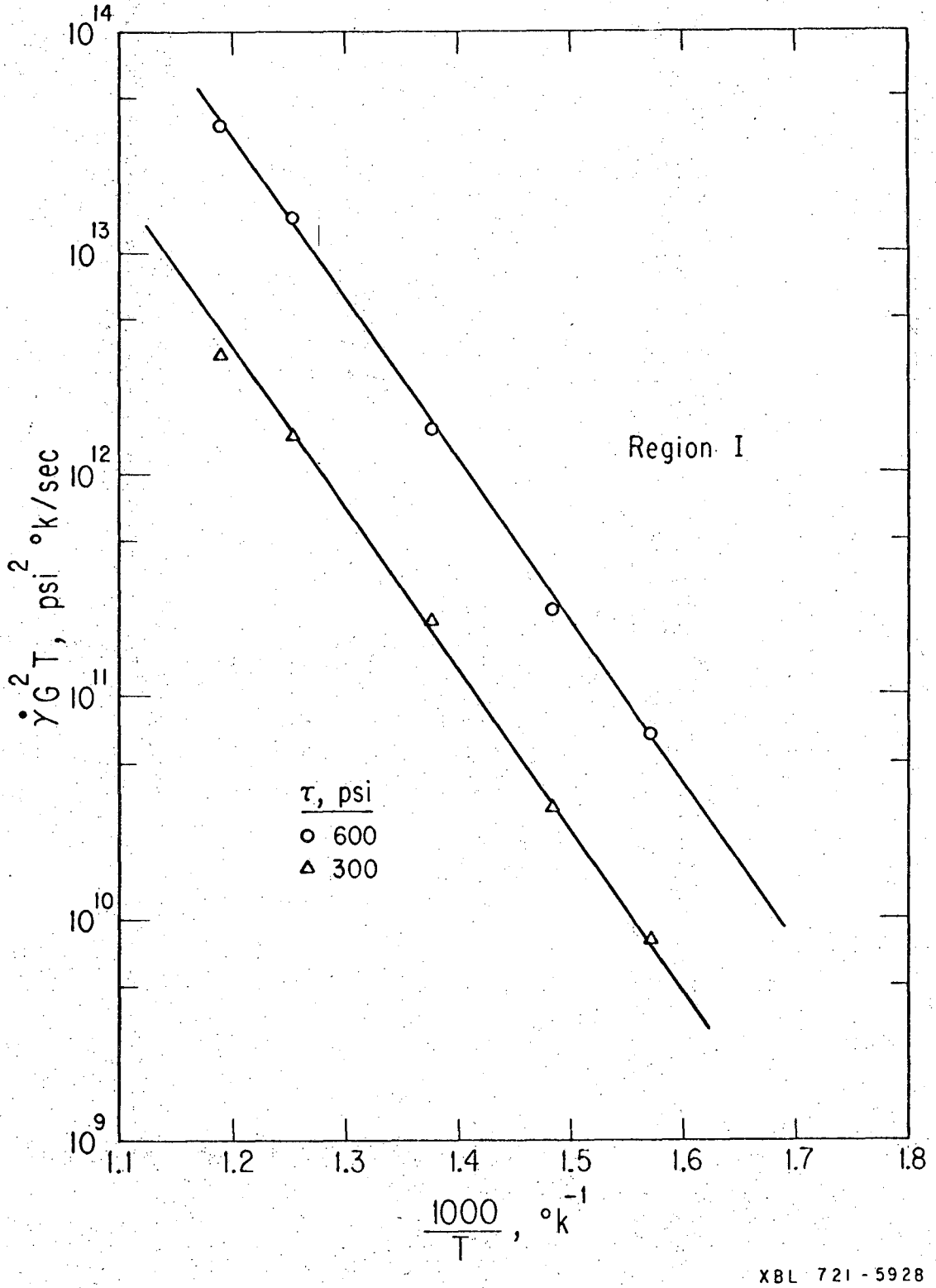
10^{14}
10^{13}
10^{12}
10^{11}
10^{10}
10^{9}
$\dot{\gamma} G^2 T$, psi^2 °k/sec
Region I
τ, psi
o 600
Δ 300
1.1
1.2
1.3
1.4
1.5
1.6
1.7
1.8
$\frac{1000}{T}$, °k^{-1}
XBL 721-5928

Fig. 3a

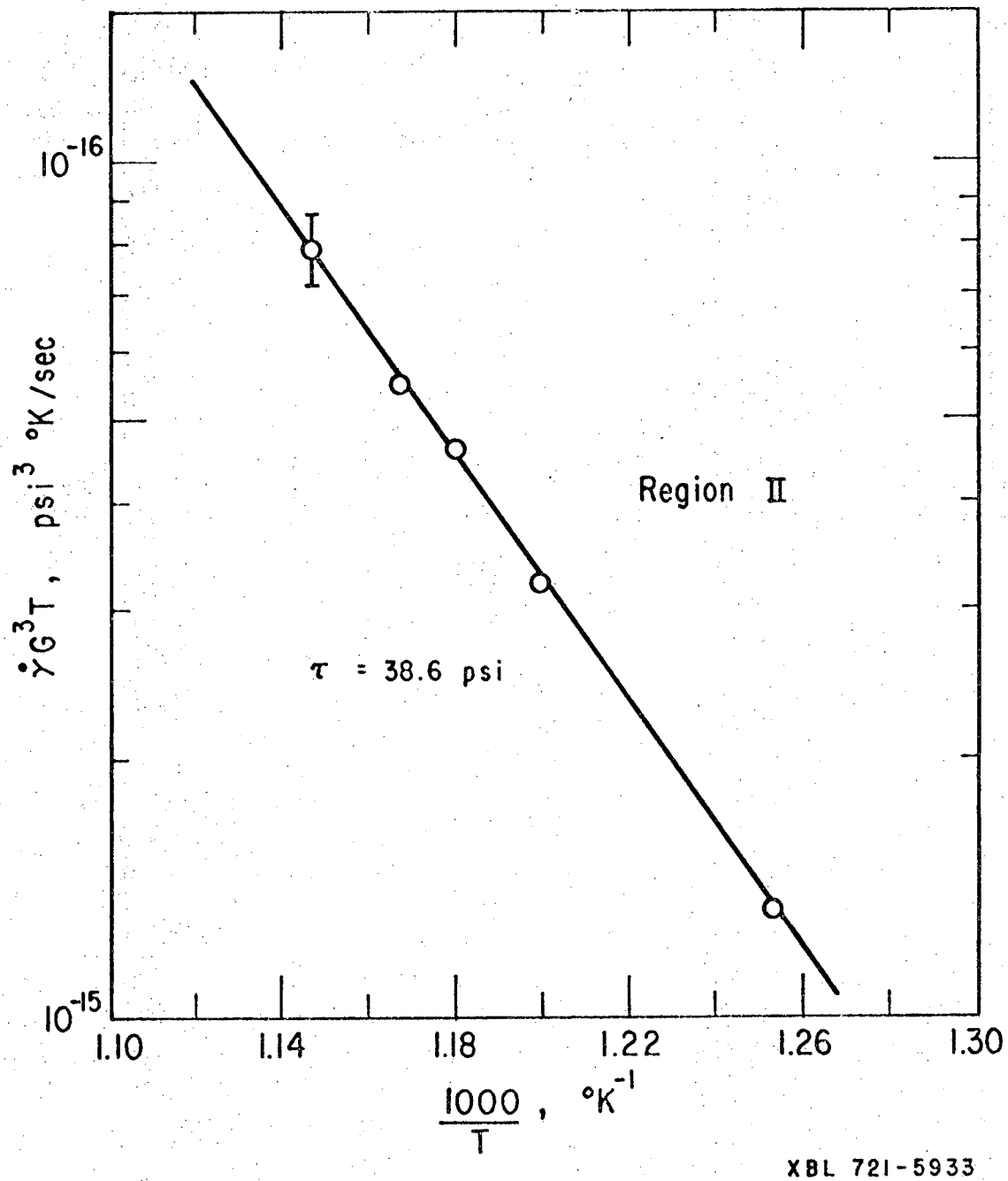
10^{-16}
10^{-15}
$\dot{\gamma} G^3 T$, psi^3 °K/sec
Region II
τ = 38.6 psi
1.10
1.14
1.18
1.22
1.26
1.30
$\frac{1000}{T}$, °K^{-1}
XBL 721-5933

Fig. 3b

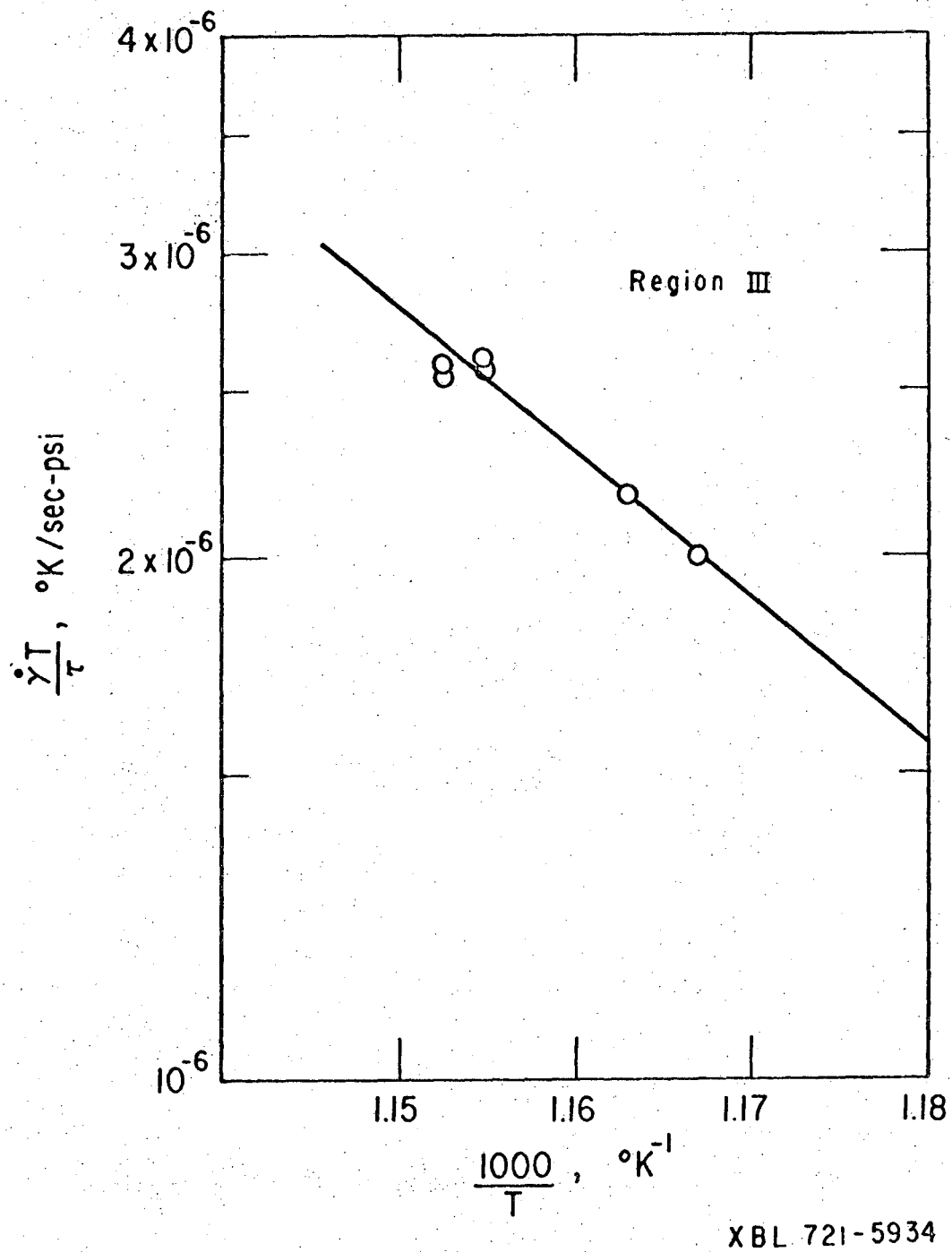
4 x 10^-6
3 x 10^-6
2 x 10^-6
10^-6
Region III
γ̇T/τ, °K/sec-psi
1.15
1.16
1.17
1.18
1000/T, °K^-1
XBL 721-5934

Fig. 3c

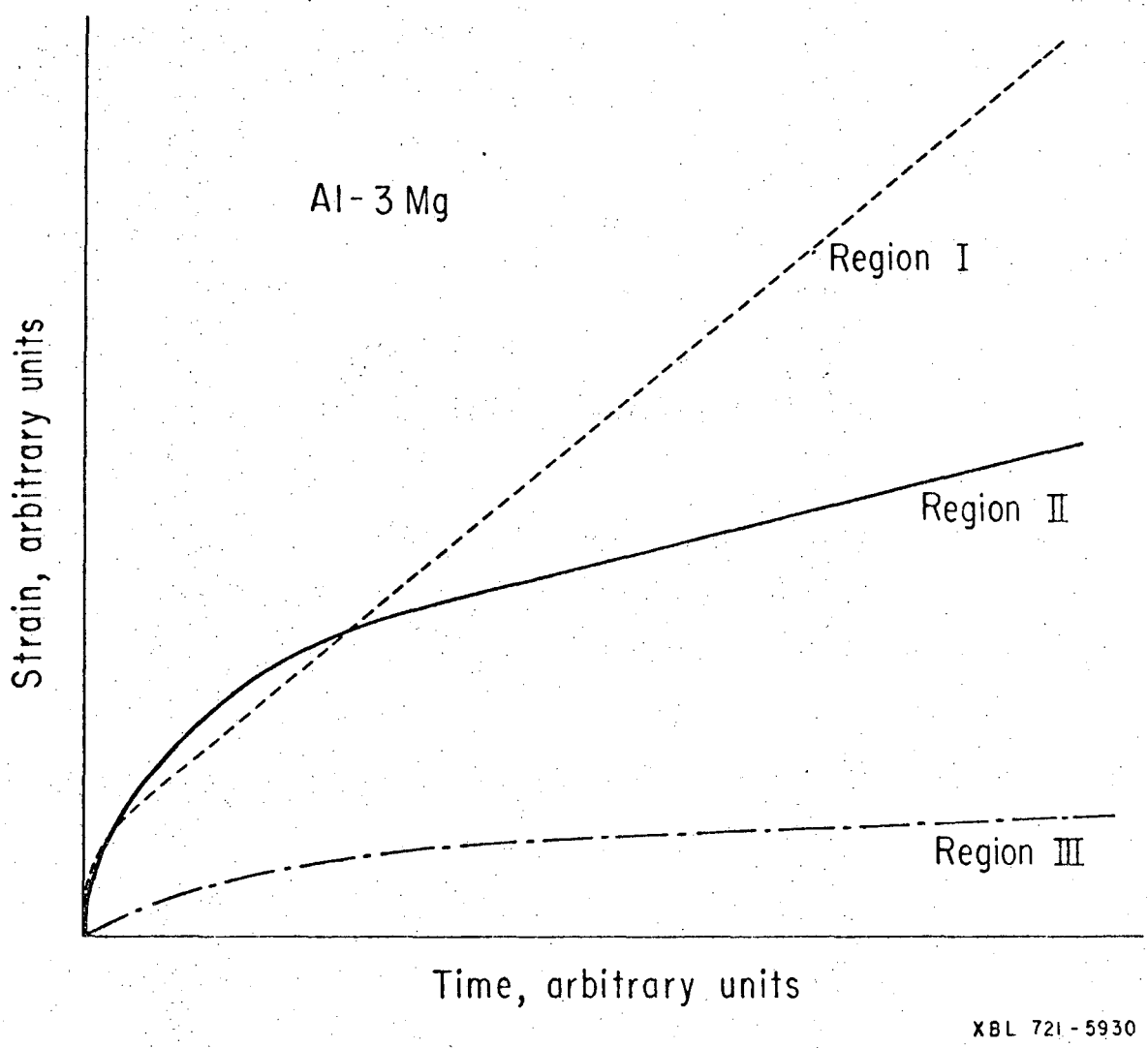
Al - 3 Mg
Region I
Region II
Region III
Strain, arbitrary units
Time, arbitrary units
XBL 721 - 5930

Fig. 4

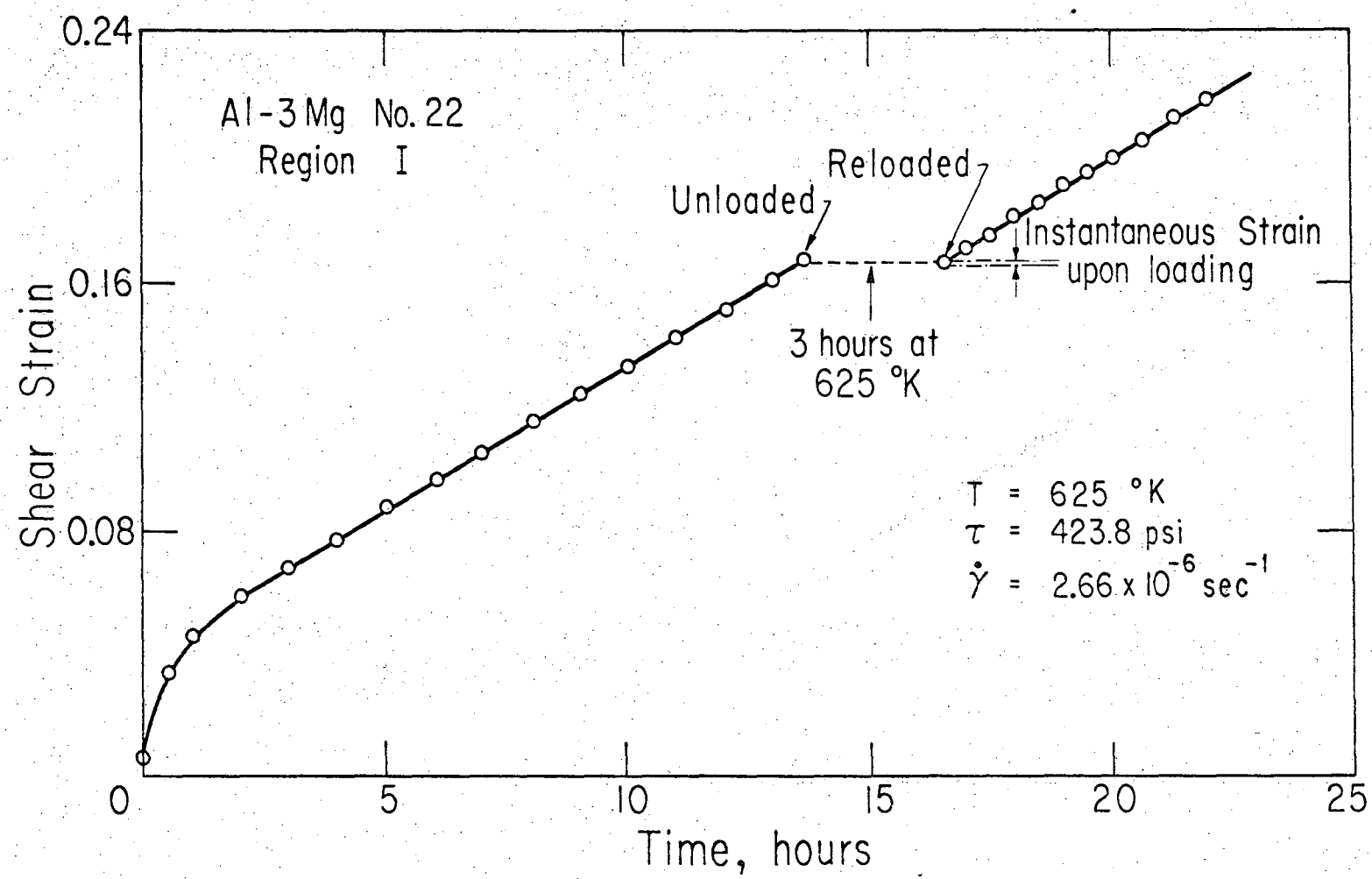
0.24
0.16
0.08
0
Shear Strain
Al-3 Mg No. 22
Region I
Unloaded
Reloaded
Instantaneous Strain
upon loading
3 hours at
625 °K
T = 625 °K
τ = 423.8 psi
γ̇ = 2.66 x 10^-6 sec^-1
5
10
15
20
25
Time, hours
XBL 721-5931

Fig. 5a

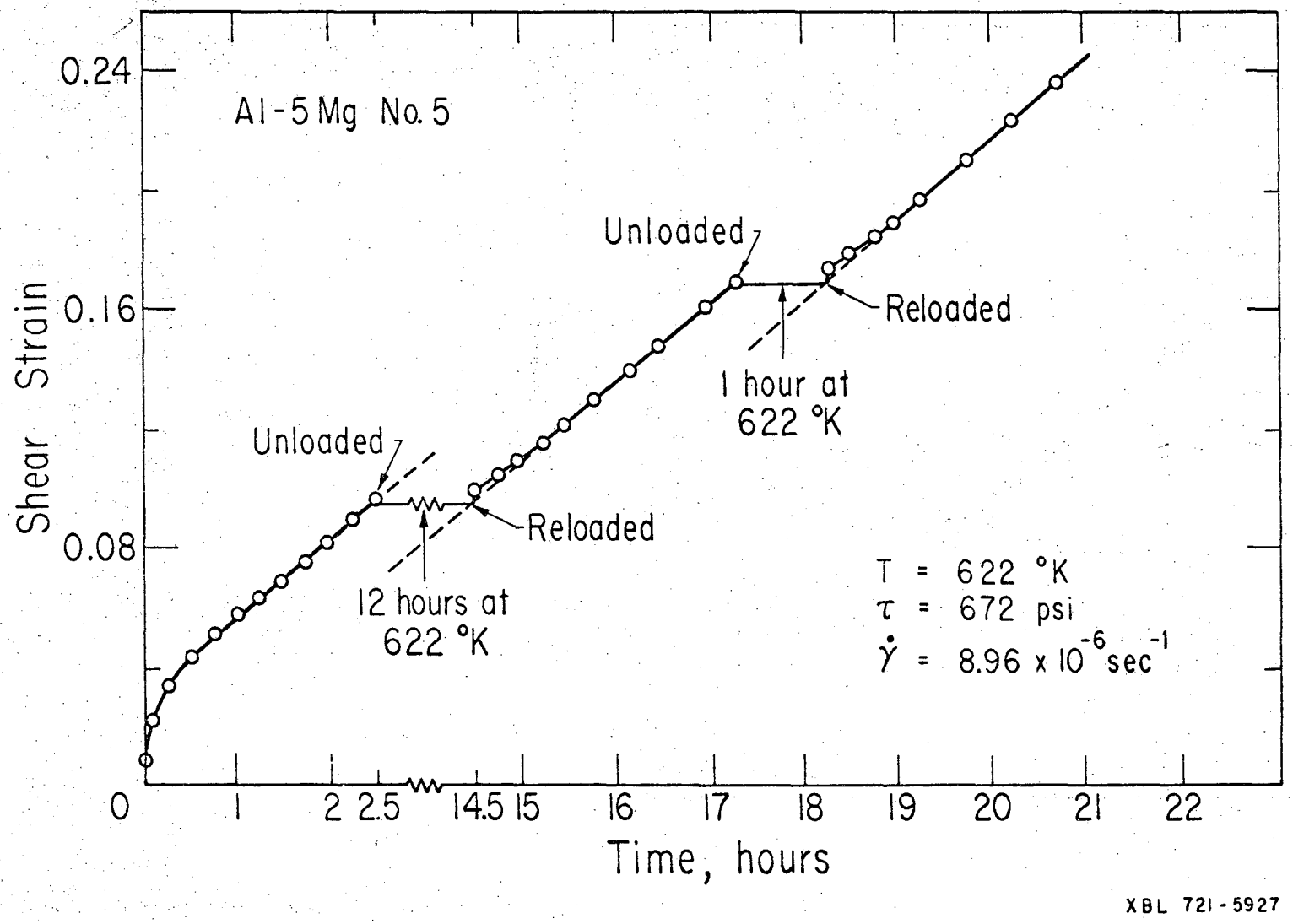
Al-5 Mg No. 5
Shear Strain
0.24
0.16
0.08
0
Unloaded
Reloaded
1 hour at
622 °K
Unloaded
Reloaded
12 hours at
622 °K
T = 622 °K
τ = 672 psi
$\dot{\gamma}$ = 8.96 x 10^{-6} sec^{-1}
1
2
2.5
14.5
15
16
17
18
19
20
21
22
Time, hours
XBL 721-5927

Fig. 5b

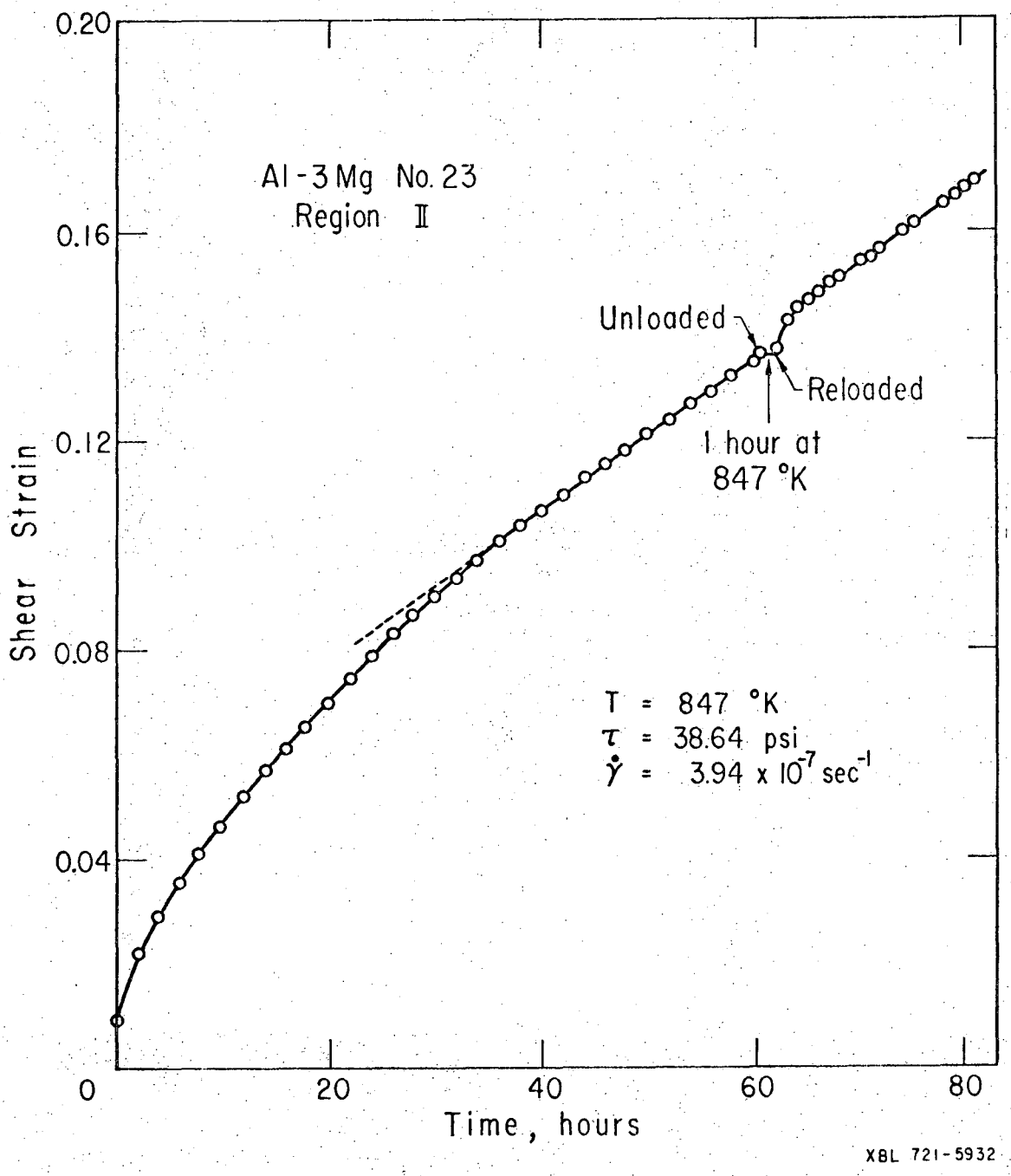
Al - 3 Mg No. 23
Region II
Unloaded
Reloaded
1 hour at
847 °K
T = 847 °K
τ = 38.64 psi
γ̇ = 3.94 x 10⁻⁷ sec⁻¹
Shear Strain
0.20
0.16
0.12
0.08
0.04
0
20
40
60
80
Time, hours
XBL 721-5932

Fig. 6

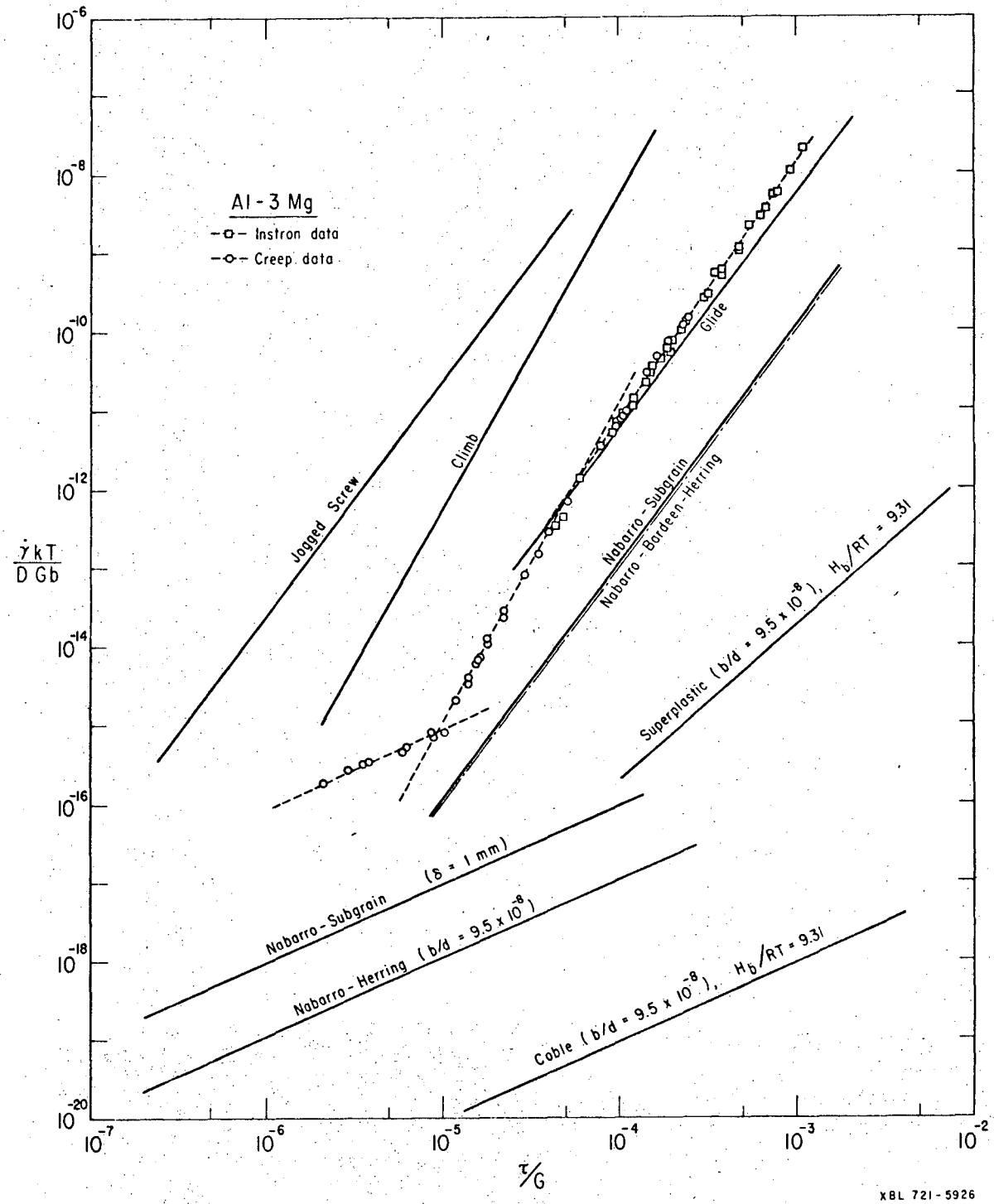
Al - 3 Mg
Instron data
Creep data
Jogged Screw
Climb
Glide
Nabarro - Subgrain
Nabarro - Bardeen - Herring
Superplastic (b/d = 9.5 x 10⁻⁸), Hb/RT = 9.31
Nabarro - Subgrain (δ = 1 mm)
Nabarro - Herring (b/d = 9.5 x 10⁻⁸)
Coble (b/d = 9.5 x 10⁻⁸), Hb/RT = 9.31
γ̇ kT / D Gb
τ/G
XBL 721-5926

Fig. 7

TECHNICAL INFORMATION DIVISION
LAWRENCE BERKELEY LABORATORY
UNIVERSITY OF CALIFORNIA
BERKELEY, CALIFORNIA 94720